Equilibrium of Interdependent Gas and Electricity Markets with Marginal Price Based Bilateral Energy Trading

Cheng Wang, Wei Wei, *Member, IEEE*, Jianhui Wang, *Senior Member, IEEE*, Lei Wu, *Senior Member, IEEE*, Yile Liang, *Student Member, IEEE*

***Abstract*— The increasing interdependencies between natural gas systems and power systems create new business opportunities in coupled energy distribution markets. This paper studies the marginal price based bilateral energy trading on the equilibrium of coupled natural gas and electricity distribution markets. Convex relaxation is employed to solve a multi-period optimal power flow problem, which is used to clear the electricity market. A successive second-order cone programming (SOCP) approach is utilized to solve a multi-period optimal gas flow problem, which is used to clear the gas market. In addition, the line pack effect in the gas network is considered, which can offer storage capacity and provide extra operation flexibility for both networks. In both problems, locational marginal energy prices are recovered from the Lagrangian multipliers associated with nodal balancing equations. Furthermore, a best-response decomposition algorithm is developed to identify the equilibrium of the coupled energy markets with bilateral gas and electricity trading, which leverages the computational superiority of SOCPs. Cases studies on two test systems validate the proposed methodology.**

***Index Terms*—interdependency, nodal energy price, natural gas network, optimal energy flow, power distribution network.**

NOMENCLATURE

A. Indices and Sets

$c \in C$	Gas compressors (gas active pipelines)
$d_g \in D_g$	Gas distribution network (GDN) loads
$d_p \in D_p$	Power distribution network (PDN) loads
$g \in G$	Gas-fired distributed generators (DGs)
$i_g \in I_g$	GDN nodes
$i_p \in I_p$	PDN buses
$l_g \in L_g$	Gas passive pipelines
$l_p \in L_p$	PDN lines
$n \in N$	Non-gas DGs
$t \in T$	Time periods
ϕ_g	Mapping between gas-fired DG and GDN node
φ_c	Mapping between compressor and PDN node

B. Parameters

$e^M_{l_p}$	PDN line current capacity
F_{l_g}, F_c	Pipeline friction coefficients
P^L_n/P^M_n	Active power range of non-gas DGs
P^L_g/P^M_g	Active power range of gas-fired DGs
a_{i_p}/b_{i_p}	Shunt condunctance/susceptance from i_p to ground
P_{d_pt}/Q_{d_pt}	PDN active/reactive power demands
Q^L_n/Q^M_n	Reactive power range of non-gas DGs
Q^L_g/Q^M_g	Reactive power range of gas-fired DGs
$Q_n(\cdot)$	Generation cost of non-gas DGs
R_{l_g}, R_c	Pipe diameters
r_{l_p}/x_{l_p}	PDN line resistance/reactance
T_k	Temperature
$v^L_{i_p}/v^M_{i_p}$	PDN bus voltage magnitude range
X_{l_g}, X_c	Length of the pipeline
Y_{d_gt}	GDN loads
y^b_m	Maximal allowed gas purchase
y^{max}_c	Maximal allowed gas in flow of compressor
Z_{lcrt_g}, Z_c	Compression factor of the pipeline
α_c	Fuel consumption coefficient of compressor
β_{i_pt}	Locational marginal electricity price
χ	Thermal equivalent conversion constant
η_g	Efficiency of gas-fired DG
γ_c	Compression factor of the compressor
λ_{gt}	Gas purchase price at a higher-level market
λ_{pt}	Power purchase price at a higher-level market
μ	Specific gas constant
ϕ_{l_g}	Weymouth equation coefficient
ρ_0	Gas density in standard condition
$\tau^u_{i_g}/\tau^l_{i_g}$	Gas pressure range
θ_g	Gas-electricity conversion factor
ϱ_{i_gt}	Locational marginal gas price
ξ	Unit transformation constant

C. Variables

e_{l_pt}	Line current square of PDN
m_{l_gt}, m_{ct}	Average gas mass of GDN
p^b_t/q^b_t	Purchased active/reactive power
p_{gt}, p_{nt}	Active power of DGs

This work is supported in part by the National Natural Science Foundation of China (51725702, 51627811), and in part by the "111" project (B08013). W. Wei's work is supported in part the Foundation for Innovative Research Groups of the National Natural Science Foundation of China (51621065). J. Wang's work is supported by the U.S. Department of Energy (DOE)'s Office of Electricity Delivery and Energy Reliability. L. Wu's work is supported in part by the U.S. National Science Foundation grant CMMI-1635339. (*Corresponding to: Wei Wei)*

C. Wang is with the State Key Laboratory of Alternate Electrical Power System with Renewable Energy Sources, North China Electric Power University, Beijing 102206, China (e-mail: chengwang@ncepu.edu.cn).

W. Wei and Y. Liang are with the State Key Laboratory of Power Systems, Department of Electrical Engineering, Tsinghua University, 100084 Beijing, China. (e-mail: wei-wei04@mails.tsinghua.edu.cn; yileat17@163.com)

J. Wang is with the Department of Electrical Engineering at Southern Methodist University, Dallas, TX, USA and the Energy Systems Division at Argonne National Laboratory, Argonne, IL, USA (email: jianhui.wang@ieee.org).

L. Wu is with the Department of Electrical and Computer Engineering at Clarkson University, Postdam, NY, 13699, USA. (e-mail: lwu@clarkson.edu).

pf_{l_pt}/qf_{l_pt}	Active/reactive power of PDN lines
q_{gt}, q_{nt}	Reactive power of DGs
u_{i_gt}	Nodal gas pressure
y_t^b	Purchased gas
$y_{l_gt}^{in}/y_{l_gt}^{out}$	Gas in/out-flow of passive pipeline
y_{ct}^{in}/y_{ct}^{out}	Gas in/out-flow of active pipeline
ν_{i_pt}	Bus voltage square of PDN

D. Acronyms

CCP	Convex concave procedure
DG	Distributed generator
GDN	Gas distribution network
GTN	Gas transmission network
LDC	Local distribution company
LMP	Locational marginal price
LMEP	Locational marginal electricity price
LMGP	Locational marginal gas price
LP	Linear prog
MILP	Mixed integer linear programming
OPF	Optimal power flow
OGF	Optimal gas flow
PDE	Partial differential equation
PDN	Power distribution network
PTN	Power transmission network
P2G	Power-to-gas
SOC	Second-order cone
SOCP	Second-order cone programming
TLEM	Transmission-level electricity market
TLGM	Transmission-level gas market

I. Introduction

THe interdependencies between power and natural gas systems have been significantly enhanced during the past decades, due to the proliferation of gas-fired generators in power systems and the emerging power-to-gas (P2G) facilities in gas systems. Such increased interdependencies not only bring potential economic and environmental benefits to the society, but also provide extra operating flexibility to both critical energy infrastructures. Many valuable works have been focused on the coordinated operation of coupled gas and power systems. Just to name a few, the optimal gas-power flow is studied in [1]; an interval optimization based robust dispatch model considering uncertain wind power and demand response is discussed in [2]; the coordinated system scheduling considering gas system dynamics is analyzed in [3]; a security-constrained co-planning model is presented in [4].

The wide deployment of gas-fired generators, gas compressors, and P2G facilities creates notable interdependencies across power systems and gas systems, as well as the markets of both energy resources. On the one hand, the electricity price will affect the gas production costs and delivery costs (because both the P2G facilities and the compressors are driven by electricity), thus will further influence the electricity demands from the gas side as well as the locational marginal gas prices (LMGPs), if a marginal pricing scheme is adopted in the gas market; on the other hand, the LMGPs will impact the production costs of the gas-fired generators, hence will influence the gas demands from the power grid and the locational marginal electricity prices (LMEPs). Some inspiring works which endeavour to address the correlation between electricity and gas markets have been found. The optimal bidding problem of the gas-fired generators in the day-ahead electricity market considering the security constraints of the gas network is discussed in [5] while neglecting the line pack effect, the quantity of natural gas contained in a certain segment of a pipeline [6]. [7] extends the work of [5] by taking unit commitment and wind power uncertainty into account. In [8], the interdependency of power and gas systems under market environment in a medium-long time horizon is analyzed, where operation costs of individual systems are optimized. Nevertheless, due to the existence of the nonlinear and nonconvex Weymouth equations, which are used for capturing the mathematical relationship between gas flows and pressures, pricing natural gas is still difficult, especially when the marginal pricing scheme is adopted. The reason is the nonconvexities will induce non-zero duality gap between the primal and dual problems and the dual variables of the nodal energy balancing equation cannot be regarded as the locational marginal prices (LMPs) directly. To conquer this obstacle, [5] relaxes the Weymouth equation as an inequality, and then uses a series of linear inequalities to approximate the relaxed inequality, resulting in a linear form of the optimal gas flow (OGF) problem. However, this treatment cannot guarantee feasibility of the OGF problem, which has been reported in literature [9], making their work less attractive. Another possible way is to add a series of binary variables and approximate the Weymoth equation by a series of linear segments, turning the gas market clearing problem into a mixed integer linear programming (MILP). It should be noted this approach has been widely adopted in the coordinated operation issues of gas-power system [10]–[14], yet hasn't been reported by any gas pricing literature. However, the approximated gas flow model is still nonconvex, due to the introduction of binaries, which call for additional pricing schemes similar with the convex hull pricing in power markets [15], [16].

Currently, the electricity and gas markets in the U.S. are cleared asynchronously [17] with different frequencies: the LMEPs are updated hourly, while the flat daily gas prices are provided for certain users. For industrial gas-fired generators, they usually get the cheapest gas price with interruptible supply contracts, which may lead to fuel inadequacy if congestion or gas shortage occurs [18]. The wide adoption of energy transition facilities and increasingly prominent system interdependencies call for more reliable and resilient operation of both networks, and also create new business opportunities that allow bilateral energy trading as well as promote the synchronization and coordination of electricity and gas markets, pioneered by the work in [17]. The first step for deregulating the gas network is to establish gas pricing policies and gas markets. We envision a pool-based gas market with LMGPs which is similar to most existing power markets, because marginal pricing scheme has been well acknowledged for its fairness and ability to price congestions. This paper studies a coupled gas-electricity market of distribution networks with bilateral energy trading at locational marginal prices. Compared the existing works, the salient features of our work are summarized as below.

1) We envision marginal gas pricing in the natural gas system. A convex optimization based method is proposed to clear the gas market and retrieve price, which overcome the computational difficulty brought by the non-convex Weymouth equations.
2) To the best of our knowledge, it is the first time that such a bilateral gas-electricity market is proposed, where the two markets trade energy at locational marginal prices. The proposed framework has the potential to promote gas and power system integration, and to increase the operational flexibility of both systems. A best-response decomposition algorithm is suggested to compute the equilibrium of the coupled energy markets, and the existence of equilibrium is discussed through the price-demand curves.

The rest of this paper is organized as follows. The market framework and basic settings are clarified in Section II, following which the mathematical formulations of the power market clearing and gas market clearing problems are elaborated. The solution methods for both market clearing problems, the calculation of LMEPs and LMGPs, and the best response algorithm for the market equilibrium are introduced in Section III. To validate the proposed model and algorithm, numerical results on two testing systems are presented in Section IV. Finally, conclusions are drawn in Section V.

II. Market Framework, OPF and OGF Problems

A. The Pool-based Market Framework

At the electricity side, the power distribution network (PDN) is connected with an upper-level power transmission network (PTN), and purchases electricity from it. Local generators in the PDN include gas-fired and non-gas distributed generators (DGs). The PDN loads are deterministic. In the OPF problem, the electricity demands from compressors are treated as parameters in the clearing process of the electricity market, which are submitted by the gas system operator; natural gas is offered at the LMGPs. The PDN operator clears the electricity market with minimal production costs, and determines the generation schedules, the gas demands, and the LMEPs simultaneously.

At the gas side, the gas distribution network (GDN) is connected with an upper-level gas transmission network (GTN), and purchases natural gas from it. The GDN loads are also considered deterministic. In the OGF problem, the natural gas demands from gas-fired units are treated as parameters in the clearing process of the gas market, which are submitted by the power system operator; electricity is supplied at the LMEPs. The GDN operator clears the gas market with minimal production costs, and determines the gas transactions, the compressor electricity usage, and the LMGPs simultaneously. The schematic diagram of the coupled energy markets is shown in Fig. 1.

The proposed market framework is designed for short-term operation of the coupled energy networks, and the corresponding market clearing models are multi-period ones. For the day-ahead market, the time period could be 1 hour, and for the intra-day market, the time period could be 15 or 5 minutes. The adpativity of the market timeframe and length of a time period can be achieved by adjusting the value of ξ, which is the unit transformation constant. In the current work, the proposed market framework mainly focuses on energy trading, and the energy transportation rights are not considered.

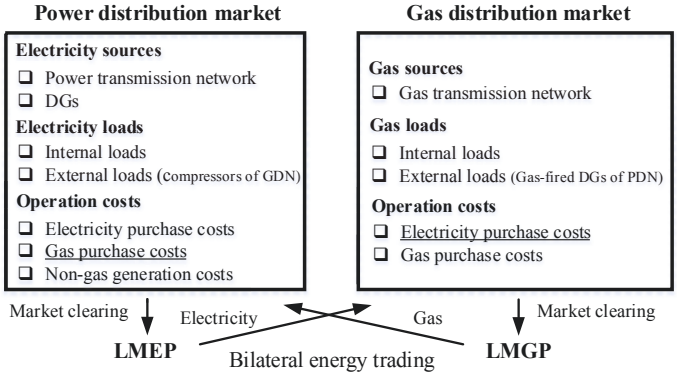

Fig. 1. The proposed coupled markets framework.

B. Assumptions and Simplifications

The main assumptions made in the proposed optimal energy flow models are clarified as follows.

1) General assumptions: (i) We are focusing on the networks and markets in the distribution level, where the PDN and the GDN are operated with radial topologies, and energy flow directions can be determined in advance. (ii) The electricity and gas consumptions are paid at locational marginal prices, i.e., the LMEPs and the LMGPs, respectively. (iii) P2G facilities are not considered in the proposed models for simplicity. Technically, the proposed models can be easily extended to ones with P2G facilities if linear P2G models are adopted [13], [19]. (iv) The PDN and GDN are owned and operated by different local distribution companies (LDCs). If not, the proposed bilateral energy trading market framework may not work and no equilibrium exists, as there is only one "player" in the integrated energy market, suggesting a holistic optimization model similar as the works of [1]–[4]. (v) The demands in both markets are non-elastic. For detailed price-responsive load model, one can refer to [20]. (vi) Only energy transactions with wholesale market are considered and there is no retail market in the current work. Nonetheless, most results in this paper are easily extendable for transmission-level studies, despite a somehow different energy flow model.

2) For the PDN: (i) Electricity can be produced locally, or purchased from the PTN at the contract prices. (ii) The branch flow model in [21] and the conic relaxation techniques in [22] are used. Reverse power flow is prohibited to guarantee the feasibility of the optimal power flow (OPF) solution obtained from the convexified model [23]–[25]. For controllable DGs, namely gas-fired DGs and diesel DGs, the assumption can be easily satisfied due to their high operation flexibility. For renewable DGs, the assumption would still hold, if curtailment is allowed. (iii) Gas demands of the gas-fired DGs solely depend on their active power outputs. (iv) We assume that unit commitment decisions have been made in a previous stage. If a DG is shut down, its output is enforced at zero. Interested readers can refer to [26] for the market clearing problem considering operating status of generators, however, this will

significantly intensifies the computation complexity. (v) DGs are assumed to be non-strategic, which means they offer their generation costs as well as capacities to the power distribution market operator directly. (vi) The PDN is assumed to be a balanced one, and then the three-phase PDN model can be replaced by an equivalent single-phase one. (vii) For each PDN node equipped with one or several DGs, there exists at least one combination of its downstream DGs, whose minimum outputs is smaller than the sum of downstream demands of the same PDN node. It should be noted the downstream DGs and loads of the PDN node include the ones connected to it if there are any. To model an OPF of meshed transmission network, the direct current flow approximation or the traditional bus-injection model can be used. The former gives rise to a linear program, and the latter is nonlinear and non-convex, but can be solved by the semi-definite relaxation method in [27].

3) For the GDN: (i) Gas flow dynamics are approximated by algebraic equations. Details can be found in [11]. (ii) A simplified and tractable compressor model in [6] is adopted, which can also be found in [10]–[13], [28], [29]. For the detailed compressor model, please refer to [30]. Please note that the accurate compressor modelling would impose great challenge on computation efficiency and model tractablity. Therefore, approximations and simiplifications in compressor modelling are quite common [10]–[14], [28], [29], [31]. A more accurate and tractable compressor model in gas network optimization problems is desired. (iii) All the compressors are driven by electricity and their cost functions are linear. According to [32] and [33], a compressor typically consumes about 3-5% of the transported gas. Likewise, the compressors are assumed to be non-strategic, which means they report their operating costs to the gas distribution market operator directly.

Remark 1: In this paper, the GDN is assumed to be operated with radial topology, which can be reasoned and supported by the following factors.

1) Practicality. There are controllable valves in the GDN, which enables the GDN to be operated with radial topology [34].
2) Efficiency. Radial-topology distribution networks enjoy high efficiency, especially in single source cases, as their total lengths of the networks are smaller than those of the meshed ones [34], [35].

Radial-topology GDN analysis can be found in many literatures [36]–[39], which further confirm the rationality of the proposed assumption. Nevertheless, the proposed model and algorithm also apply to meshed network if gas flow directions can be specified in advance from heuristic methods or operating experiences. We do not actually require that gas flow directions keep unchanged all day long. In fact, gas flow problem is hard to solve for non-radial networks, even under steady-state and balanced conditions [40], due to the nonlinearities and nonconvexities in the gas network model, let along the OGF problem. Tractable pricing schemes for the meshed GDNs would be the one of the future works.

C. Power Distribution Market Clearing

The PDN is connected to a upper-level power transmission network (PTN), which serves as a power supplier with infinite capacity. The PDN is a price-taker and pays the energy transaction costs to the transmission level electricity market according to the electricity price. In the electricity market, the operator aims to minimize the production costs, leading to the following OPF problem

$$\min_{\Phi_p} \sum_t \Big(\sum_g \frac{\varrho_{i_g t} p_{gt}}{\eta_g \theta_g} + \sum_n Q_n(p_{nt}) + \lambda_{pt} p_t^b\Big),\ i_g \in \phi_g^{-1}$$
$$\Phi_p = \{e_{i_p t}, p_t^b, p_{gt}, p_{nt}, q_t^b, q_{gt}, q_{nt}, pf_{l_p t}, qf_{l_p t}, v_{i_p t}\} \tag{1}$$

$$s.t. \quad 0 \le e_{l_p t} \le (e_{l_p}^M)^2,\ \forall l_p, \forall t, \tag{2}$$

$$(v_{i_p}^L)^2 \le \nu_{i_p t} \le (v_{i_p}^M)^2,\ \forall i_p, \forall t, \tag{3}$$

$$P_{\{\cdot\}}^L \le p_{\{\cdot\}t} \le P_{\{\cdot\}}^M,\ \{\cdot\} = \{g, n\}, \forall t, \tag{4}$$

$$Q_{\{\cdot\}}^L \le q_{\{\cdot\}t} \le Q_{\{\cdot\}}^M,\ \{\cdot\} = \{g, n\}, \forall t, \tag{5}$$

$$p_t^b \ge 0,\ q_t^b \ge 0,\ \forall t, \tag{6}$$

$$pf_{l_p t} \ge 0,\ qf_{l_p t} \ge 0, \forall l_p, t, \tag{7}$$

$$\begin{aligned} &\sum_{\{\cdot\} \in \Psi_{\{\cdot\}}(i_p)} p_{\{\cdot\}t} + \sum_{l \in \Psi_{O_2}(i_p)} (pf_{l_p t} - r_{l_p} e_{l_p t}) - a_{i_p} \nu_{i_p} \\ &- \sum_{l \in \Psi_{O_1}(i_p)} pf_{l_p t} - \sum_{d_p \in \Psi_{d_p}(i_p)} P_{d_p t} + 1_{\{i_p = i_p^0\}} p_t^b \\ &- \sum_{c \in \Psi_c(i_p)} \chi \alpha_c y_{ct}^{in} = 0 : \beta_{i_p t},\ \{\cdot\} = \{g, n\},\ \forall i_p, t, \end{aligned} \tag{8}$$

$$\begin{aligned} &\sum_{\{\cdot\} \in \Psi_{\{\cdot\}}(i_p)} q_{\{\cdot\}t} + \sum_{l \in \Psi_{O_2}(i_p)} (qf_{l_p t} - x_{l_p} e_{l_p t}) - b_{i_p} \nu_{i_p} \\ &- \sum_{l \in \Psi_{O_1}(i_p)} qf_{l_p t} - \sum_{d_p \in \Psi_{d_q}(i_p)} Q_{d_q t} + 1_{\{i_p = i_p^0\}} q_t^b \\ &= 0,\ \{\cdot\} = \{g, n\},\ \forall i_p,\ \forall t, \end{aligned} \tag{9}$$

$$\begin{aligned} \nu_{i_{p2} t} = \nu_{i_{p1} t} &- 2(r_{l_p} pf_{l_p t} + x_{l_p} qf_{l_p t}) \\ &+ (r_{l_p}^2 + x_{l_p}^2) e_{l_p t},\ \forall (i_{p1}, i_{p2}) \in l_p, \forall t, \end{aligned} \tag{10}$$

$$\nu_{i_{p1} t} e_{l_p t} \ge pf_{l_p t}^2 + qf_{l_p t}^2,\ \forall (i_{p1}, i_{p2}) \in l_p, \forall t. \tag{11}$$

In this formulation, the objective function (1) is the total operating costs of the PDN, in which the first two components are the generation costs of gas-fired DGs and non-gas DGs, respectively, and the third one is the energy transaction costs paid to the transmission-level electricity market (TLEM); Φ_p collects decision variables of the OPF problem. (2) and (3) impose boundaries for line currents and bus voltages. (4) and (5) enforce active and reactive generation capacities for DGs. (6) and (7) ban reverse energy transactions and power flows, respectively. (8) and (9) are the nodal power balancing equations, where $\Psi_g(i_p)$, $\Psi_n(i_p)$, $\Psi_{d_p}(i_p)$, and $\Psi_c(i_p)$ stand for sets of gas-fired DGs, non-gas DGs, electricity loads, and gas compressors connecting to node i_p; Ψ_{O_1} (Ψ_{O_2}) stands for the set of feeders whose head (tail) node is i_p; i_p^0 is the connection node between the upper-level PTN and PDN. (10) is the voltage drop equation. (11) defines the relaxed line apparent power, which can be expressed via a standard second-order cone constraint. It is proved that (11) will be

binding at the optimal solution under mild conditions [22]. Dual variables which serve as the LMEPs are indicated in (8) following a colon. In the proposed market clearing model of the PDN, renewable DGs, if there is any, use forecasted outputs. Uncertainty is not the main focus of this paper, but will be an interesting direction in future research. A relevant discussion is presented in Section III.C.

D. Gas Distribution Market Clearing

In the gas market, the operator aims to minimize the total gas production costs, leading to the following OGF problem

$$\min_{\Phi_g} \sum_t (\lambda_{gt} y_t^b + \sum_c \beta_{i_p t} \chi \alpha_c y_{ct}^{in}),\ i_p \in \varphi_c^{-1}, \tag{12}$$
$$\Phi_g = \{y_t^b, y_{l_g t}^{in}, y_{l_g t}^{out}, y_{ct}^{in}, y_{ct}^{out}, u_{i_g t}, m_{l_g t}\}$$

$$s.t.\ \ 0 \le y_t^b \le y_m^b,\ \forall t, \tag{13}$$

$$\tau_{i_g}^l \le u_{i_g t} \le \tau_{i_g}^u,\ \forall i_g, t, \tag{14}$$

$$1_{\{i_g = i_g^0\}} y_t^b + \sum_{\{\cdot\} \in \Theta_{\{\cdot\}_2}(i_g)} y_{\{\cdot\}t}^{in} - \sum_{\{\cdot\} \in \Theta_{\{\cdot\}_1}(i_g)} y_{\{\cdot\}t}^{out} = \sum_{n \in \Theta_n(i_g)} \frac{p_{gt}}{\eta_g \theta_g} + \sum_{d_g \in \Theta_{d_g}(i_g)} Y_{d_g t} : \varrho_{i_g t},\ \{\cdot\} = \{c, l_g\}, \forall i_g, t, \tag{15}$$

$$m_{\{\cdot\}t} = \frac{\pi}{4} \frac{X_{\{\cdot\}} R_{\{\cdot\}}^2}{\mu T_k Z_{\{\cdot\}} \rho_0} \frac{u_{\{\cdot\}^1 t} + u_{\{\cdot\}^2 t}}{2},\ \{\cdot\} = \{c, l_g\},\ \forall t, \tag{16}$$

$$m_{\{\cdot\}t} = m_{\{\cdot\}(t-1)} + y_{\{\cdot\}t}^{in} - y_{\{\cdot\}t}^{out},\ \{\cdot\} = \{c, l_g\},\ t = 2, \ldots, T, \tag{17}$$

$$m_{\{\cdot\}1} = m_{\{\cdot\}T} + y_{\{\cdot\}1}^{in} - y_{\{\cdot\}1}^{out},\ \{\cdot\} = \{c, l_g\}, \tag{18}$$

$$u_{c^2 t} \le \gamma_c u_{c^1 t},\ \forall c, t, \tag{19}$$

$$0 \le y_{ct}^{in} \le y_c^{max},\ \forall c, t, \tag{20}$$

$$(y_{l_g t}^{in} + y_{l_g t}^{out}) | y_{l_g t}^{in} + y_{l_g t}^{out} | = 4 \phi_{l_g} [(u_{l_g^1 t})^2 - (u_{l_g^2 t})^2],\ \forall l_g, t, \tag{21}$$

$$\phi_{l_g} = \left(\pi^2 \xi^2 R_{l_g}^5\right) / \left(16 X_{l_g} F_{l_g} \mu T_k Z_{l_g} \rho_0^2\right),\ \forall l_g. \tag{22}$$

In this formulation, the objective function (12) is the total operating costs of the GDN, in which the first component is the gas purchase costs from the transmission-level gas market (TLGM), and the second one is the operating costs of compressors. Φ_g collects decision variables of the OGF problem. (13) prevents negative or excessive gas transactions. (14) imposes boundaries for nodal gas pressures. (15) represents nodal gas balancing conditions, where $\Theta_{d_g}(i_g)$ and $\Theta_n(i_g)$ represent sets of gas loads and gas-fired DGs connecting to node i_g; $\Theta_{c_1}(i_g)$, $\Theta_{c_2}(i_g)$, $\Theta_{l_{g_1}}(i_g)$, and $\Theta_{l_{g_2}}(i_g)$ represent sets of active and passive pipelines whose head/tail node is i_g. Particularly, active/passive pipelines refer to those with/without compressors; i_g^0 denotes the connection node between the upper-level GTN and GDN. (16) gives the relationship between line pack and average pressure of a pipeline. (17) and (18) depict the time-dependent relationship between line pack and gas flow, and require the initial and final levels of line pack are the same in a clearing cycle. The mathematical procedure to derive (16) and (17) can be found in the Appendix of [11], in which a constant compressibility factor Z_{l_g} is adopted to preserve linearity. For each active pipeline, (19) and (20) limit the maximum compression ratio and gas flow, where $u_{c^1 t}$ and $u_{c^2 t}$ are the pressures of head and tail nodes of an active pipeline, respectively. (19)-(20) constitute a simplified compressor model, which has been justified and adopted in [6]. (21) is the Weymouth equation which characterizes the relationship between gas flow in a passive pipeline and nodal gas pressures, where $u_{l_g^1 t}$ and $u_{l_g^2 t}$ are pressures of head and tail nodes of l_g, respectively. (22) defines the coefficient ϕ_{l_g} in the Weymouth equation. Dual variables which serve as the LMGPs are indicated in (15) following a colon.

The non-differentiable absolute value function in (21) greatly challenges the solution of the OGF problem. Recalling the first assumption of the general ones in Section II.A, (21) can be reduced as

$$u_{l_g^1 t} \ge u_{l_g^2 t},\ \ \forall l_g,\ t, \tag{23}$$

$$y_{l_g t}^{in} + y_{l_g t}^{out} \ge 0,\ \ \forall l_g,\ t, \tag{24}$$

$$(y_{l_g t}^{in} + y_{l_g t}^{out})^2 / 4 = \phi_{l_g} ((u_{l_g^1 t})^2 - (u_{l_g^2 t})^2),\ \ \forall l_g, t. \tag{25}$$

We assume the notations of head and tail nodes of l_g are consistent with the positive direction of gas flows. (23)-(25) naturally hold for radial GDNs. The non-convexity in the OGF problem originates from equation (25).

Remark 2: According to the literature [41], [42], the cycling periods of most gas storages are years or months, which are not inconsistent with the time scale of the OGF problem tackled here. Besides, gas storages usually locate in transmission networks rather than distribution networks [42]. Therefore, in the short operation of gas distribution networks, the line pack, defined as the short-term storage by [41], acts as the distributed gas storage facilities with limited regulation capability compared with the transmission-level gas storages, which has been modelled and serves as the only gas storage in the proposed OGF model. With more interactions between distribution-level electricity and gas networks, there may be more gas storage facilities in the GDN in the future. Though gas storage facilities are not considered in this work, it can be easily incorporated in the OGF model and efficiently solved by the proposed algorithm, if it is convex mathematically. Take the simplified linear gas storage model in [2], [11]–[13] as an example:

$$\underline{y}_s^{in} \le y_{st}^{in} \le \bar{y}_s^{in},\ \forall s,\ \forall t, \tag{26a}$$

$$\underline{y}_s^{out} \le y_{st}^{out} \le \bar{y}_s^{out},\ \forall s,\ \forall t, \tag{26b}$$

$$\underline{r}_s \le r_{st} \le \bar{r}_s,\ \forall s,\ \forall t, \tag{26c}$$

$$r_{st} = r_{s,t-1} + y_{st}^{in} - y_{st}^{out},\ \forall s,\ \forall t, \tag{26d}$$

where s is the index for gas storages; $\underline{y}_s^{in}$ and $\bar{y}_s^{in}$ ($\underline{y}_s^{out}$ and $\bar{y}_s^{out}$) are the lower and upper limits of in (out) rate of gas storages, respectively; $\underline{r}_s$ and $\bar{r}_s$ are lower and upper limits of stored gas; y_{st}^{in}, y_{st}^{out}, and r_{st} are the in rate, out rate, and stored gas, respectively. In this formulation, (26a) and (26b) describe the limits for in and out rates of gas storages, respectively; (26c) imposes the boundaries for stored gas; (26d) represents the variation of stored gas. Accordingly, the

nodal gas balancing equation needs to be modified as follows

$$1_{\{i_g=i_g^0\}}y_t^b+\sum_{\{\cdot\}\in\Theta_{\{\cdot\}_2}(i_g)}y_{\{\cdot\}t}^{in}-\sum_{\{\cdot\}\in\Theta_{\{\cdot\}_1}(i_g)}y_{\{\cdot\}t}^{out}+\sum_{s\in\Theta_s(i_g)}\left(y_{st}^{out}-y_{st}^{in}\right)=\sum_{n\in\Theta_n(i_g)}\frac{p_{gt}}{\eta_g\theta_g}+\sum_{d_g\in\Theta_{d_g}(i_g)}Y_{d_gt},\ \{\cdot\}=\{c,l_g\},\forall i_g,t. \tag{27}$$

It should be noted that modeling gas storage as (26a)-(26d) will not change the mathematical property of the gas distribution market clearing problem, which means the proposed approach would still work.

Remark 3: There is no imbalance charge when the total gas supply exceeds or is less than the total gas demand in a time period in the current formulation, as constraints (17) and (18) are embedded in the proposed OGF formulation, which enforce the initial and final line pack levels of a clearing cycle are the same. However, it would be interesting to treat the line pack as an individual market product and explore its pricing scheme.

Remark 4: The formulations of gas flows are expressed by partial differential equations (PDEs), as shown in the Appendix of [11]. Then the implicit method of finite differences is used to discretize these PDEs in time and space. In [11], the time and space steps are selected as one hour and the length of the pipeline, respectively. Similarly, the current line pack model, namely (16)-(18), is an approximation of the actual one. One possible method to improve the accuracy of approximation without losing its linearity is reported in [43], which is achieved by introducing fictitious gas nodes in a pipeline and dividing one pipeline into several sub-pipelines spatially. Temporally, the approximation could also be enhanced by using smaller time steps for the line pack model compared with the one for gas market clearing.

Remark 5: Weymouth equation is adopted to approximate the gas flow in a pipeline, which is the same as [44]. In fact, Weymouth equation is widely adopted in transmission-level gas network analysis [5], [11], [13], while the pressure levels of GDNs are lower than GTNs, which means the Weymouth equation might not be the most accurate formula for distribution-level gas flow analysis. In fact, there are many formulas to describe the gas flow in a pipeline, however, none has the complete acceptance of academia and industry [45]. This is because of the effects of friction are difficult to quantify, resulting in formula variations in the literature. Therefore, more accurate and tractable formulations for distribution-level gas flow analysis are desired.

Remark 6: According to current natural gas market reality, LMGPs stay unchanged during a gas day. In the proposed gas market model, we assume the real-time natural gas pricing mechanism is adopted. However, the proposed model can be in line with current natural gas market reality after adding the nodal gas balancing equations (15) with respect to t and regarding the dual variable ϱ_{i_g} of the following equation as LMGP.

$$\sum_t\left(1_{\{i_g=i_g^0\}}y_t^b+\sum_{\{\cdot\}\in\Theta_{\{\cdot\}_2}(i_g)}y_{\{\cdot\}t}^{in}-\sum_{\{\cdot\}\in\Theta_{\{\cdot\}_1}(i_g)}y_{\{\cdot\}t}^{out}\right)=\sum_t\left(\sum_{n\in\Theta_n(i_g)}\frac{p_{gt}}{\eta_g\theta_g}+\sum_{d_g\in\Theta_{d_g}(i_g)}Y_{d_gt}\right):\varrho_{i_g},\ \{\cdot\}=\{c,l_g\},\forall i_g. \tag{28}$$

With the aforementioned modifications, the LMGPs of gas market will remain unchanged throughout a gas day.

III. Solution Methodology

A. Locational Marginal Electricity Price

The compact form of the OPF problem is given by

$$\min_{\boldsymbol{x}}\ \boldsymbol{f}^\top\boldsymbol{x}+\boldsymbol{\varrho}^\top\boldsymbol{F}_{\varrho x}\boldsymbol{x} \tag{29a}$$

$$s.t.\ \mathbf{0}\le\boldsymbol{C}_1\boldsymbol{x}+\boldsymbol{d}_1+\boldsymbol{D}_1\boldsymbol{y}\ :\ \boldsymbol{\beta}, \tag{29b}$$

$$||\boldsymbol{A}_i\boldsymbol{x}+\boldsymbol{b}_i||_2\le\boldsymbol{c}_{2,i}^\top\boldsymbol{x}+d_{2,i}\ :\ \boldsymbol{\delta},\boldsymbol{\omega},\ i\in L_p, \tag{29c}$$

where $\boldsymbol{x}$ is vector of decision variables in Φ_g; $\boldsymbol{f},\boldsymbol{F}_{\varrho x},\boldsymbol{C}_1,\boldsymbol{d}_1,\boldsymbol{D}_1,\boldsymbol{A}_i,\boldsymbol{b}_i,\boldsymbol{c}_{2,i},d_{2,i}$ are coefficient matrices corresponding to (1)-(11); $\boldsymbol{\beta},\boldsymbol{\delta}$ and $\boldsymbol{\omega}$ are dual variables. In problem (29), $\boldsymbol{y}$ and $\boldsymbol{\varrho}$ are constant electricity demands and LMGPs delivered from the GDN. The dual SOCP of (29) is given by

$$\max_{\boldsymbol{\beta},\boldsymbol{\delta},\boldsymbol{\omega}}-\boldsymbol{\beta}^\top(\boldsymbol{d}_1+\boldsymbol{D}_1\boldsymbol{y})^\top-\sum_{i\in L_p}\left(\boldsymbol{\delta}_i^\top\boldsymbol{b}_i+\omega_i d_{2,i}\right) \tag{30a}$$

$$s.t.\ \boldsymbol{f}+\boldsymbol{F}_{\varrho x}^\top\boldsymbol{\varrho}=\boldsymbol{C}_1^\top\boldsymbol{\beta}+\sum_{i\in L_p}\left(\boldsymbol{A}_i^\top\boldsymbol{\delta}_i+\boldsymbol{c}_{2,i}\omega_i\right), \tag{30b}$$

$$\boldsymbol{\beta}\ge\mathbf{0},\ \|\boldsymbol{\delta}_i\|_2\le\omega_i,\quad\forall i\in L_p. \tag{30c}$$

As long as the OPF problem (29) has a Slater point, strong duality holds, which means dual variable β_{i_pt} is the LMEP at bus i_p. Some commercial SOCP solvers, such as MOSEK, offers primal and dual optimal solutions at the same time, thus can be used to procure the OPF solution and the LMEPs more conveniently.

B. Locational Marginal Gas Price

The compact form of the OGF problem is expressed as

$$Obj_{gas}=\min_{\boldsymbol{y}}\ \boldsymbol{g}^\top\boldsymbol{y}+\boldsymbol{\beta}^\top\boldsymbol{G}_{\beta y}\boldsymbol{y} \tag{31a}$$

$$s.t.\ \ \mathbf{0}\le\boldsymbol{E}\boldsymbol{y}+\boldsymbol{h}+\boldsymbol{H}\boldsymbol{x},\ (25). \tag{31b}$$

where $\boldsymbol{y}$ is vector of decision variables in Φ_g, and $\boldsymbol{g},\boldsymbol{G}_{\beta y}$, $\boldsymbol{E},\boldsymbol{h},\boldsymbol{H}$ are coefficient matrices in (12)-(20), (22), (23)-(24). $\boldsymbol{x}$ and $\boldsymbol{\beta}$ are constants delivered from the PDN.

(31) is a non-convex program due to the quadratic equalities in (25). In view of the difference-of-convex structure in the right-hand side of (25), (31) can be solved by a convex-concave procedure (CCP) discussed in [46], whose basic idea is to linearize the concave part in the constraints. To perform CCP, (25) is written as two opposite inequalities

$$(y_{l_gt}^{in}+y_{l_gt}^{out})^2/4+\phi_{l_g}(u_{l_g^2t})^2\le\phi_{l_g}(u_{l_g^1t})^2,\ \forall l_g,t, \tag{32a}$$

$$\phi_{l_g}(u_{l_g^1t})^2\le(y_{l_gt}^{in}+y_{l_gt}^{out})^2/4+\phi_{l_g}(u_{l_g^2t})^2,\ \forall l_g,t. \tag{32b}$$

Algorithm 1 Penalty CCP for OGF

1: Initialize the penalty parameters $\pi_0, \pi_{max}, \kappa > 1$ and convergence parameters δ and ε. Set the iteration index $k = 0$. Solve the following relaxed OGF problem

$$Obj_{gas} = \min_{\boldsymbol{y}} \ \boldsymbol{g}^\top \boldsymbol{y} + \boldsymbol{\beta}^\top \boldsymbol{G}_{\beta y} \boldsymbol{y} \tag{36a}$$

$$s.t. \ \ \mathbf{0} \le \boldsymbol{E}\boldsymbol{y} + \boldsymbol{h} + \boldsymbol{H}\boldsymbol{x}, \ (33). \tag{36b}$$

The optimal solutions (values) are $\boldsymbol{y}_0$ (Obj^0_{gas}).

2: Solve the following penalized OGF problem

$$Obj_{gas} = \min_{\boldsymbol{y}} \ \boldsymbol{g}^\top \boldsymbol{y} + \boldsymbol{\beta}^\top \boldsymbol{G}_{\beta y} \boldsymbol{y} + \pi_k \mathbf{1}^\top \boldsymbol{s} \tag{37a}$$

$$s.t. \ \ \mathbf{0} \le \boldsymbol{E}\boldsymbol{y} + \boldsymbol{h} + \boldsymbol{H}\boldsymbol{x}, \ \boldsymbol{s} \ge \mathbf{0}, \ (33), \tag{37b}$$

$$\|\boldsymbol{G}_1 \boldsymbol{y} + \boldsymbol{g}_1\| \le \boldsymbol{g}_2^\top \boldsymbol{y} + \boldsymbol{g}_3, \tag{37c}$$

where coefficient matrices $\boldsymbol{G}_1, \boldsymbol{g}_1, \boldsymbol{g}_2$, and $\boldsymbol{g}_3$ in SOC constraint (37c) corresponding to (34) are updated at $\boldsymbol{y}_k$. The optimal solution is $\boldsymbol{y}_{k+1}$ and $\boldsymbol{s}_{k+1}$, with the optimal value of Obj^{k+1}_{gas}.

3: If (38a) and (38b) are satisfied, then terminate and report the optimal solution; otherwise, update $k = k+1$, $\pi_{k+1} = \min(\kappa \pi_k, \pi_{max})$, and go to Step 2.

$$|Obj^{k+1}_{gas} - Obj^k_{gas}| \le \delta, \tag{38a}$$

$$s_{l_g t, k+1} \le \varepsilon \cdot \phi_{l_g} (u_{l^1_g t})^2, \ \forall l_g, t. \tag{38b}$$

Algorithm 2 Best-Response Decomposition

1: Set $\varrho_{i_g t} = \lambda_{gt}$ and $y^{in}_{ct} = 0$. Set the maximum iteration number j^{max} and convergence criterion ϵ. Set $j = 1$.

2: Solve the OPF problem (29) with given y^{in}_{ct}, $\varrho_{i_g t}$, and obtain p^j_{gt}. Solve problem (30), and obtain LMEP $\beta^j_{i_p t}$.

3: Solve the OGF problem (31) using Algorithm 1 with given p^j_{gt}, $\beta^j_{i_p t}$, and obtain $y^{in,j}_{ct}, \mathcal{M}^{k,j}_g$. Solve the dual problem of $\mathcal{M}^{k,j}_g$, and obtain LMGP $\varrho^j_{i_g t}$.

4: If following criteria are met, terminate and report p^j_{gt}, $\beta^j_{i_p t}$, $y^{in,j}_{ct}$, $\varrho^j_{i_g t}$; else if $j = j^{max}$, terminate and report failure of convergence; else, update $j = j + 1$, and go to Step 2.

$$|p^j_{gt} - p^{j-1}_{gt}| \le \epsilon \cdot \max\{p^j_{gt}, p^{j-1}_{gt}\}, \ \forall g, t,$$

$$|\beta^j_{i_p t} - \beta^{j-1}_{i_p t}| \le \epsilon \cdot \max\{\beta^j_{i_p t}, \beta^{j-1}_{i_p t}\}, \ \forall i_p, t,$$

$$|y^{in,j}_{ct} - y^{in,j-1}_{ct}| \le \epsilon \cdot \max\{y^{in,j}_{ct}, y^{in,j-1}_{ct}\}, \ \forall c, t,$$

$$|\varrho^j_{i_g t} - \varrho^{j-1}_{i_g t}| \le \epsilon \cdot \max\{\varrho^j_{i_g t}, \varrho^{j-1}_{i_g t}\}, \ \forall i_g, t.$$

Because $u_{l^1_g t}$ and ϕ_{l_g} are positive, $\sqrt{\phi_{l_g}} u_{l^1_g t} \ge 0$ holds, and (32a) is equivalent to SOC inequalities shown below

$$\left\| \begin{array}{c} (y^{in}_{l_g t} + y^{out}_{l_g t})/2 \\ \sqrt{\phi_{l_g}} u_{l^2_g t} \end{array} \right\| \le \sqrt{\phi_{l_g}} u_{l^1_g t}, \ \forall l_g, t. \tag{33}$$

Furthermore, given the value of $u_{l^2_g t,k}, y^{in}_{l_g t,k}$ and $y^{out}_{l_g t,k}$, (32b) can be convexified by replacing the right-hand side with its linear approximation, yielding

$$\begin{aligned} \phi_{l_g} (u_{l^1_g t})^2 \le & \frac{(y^{in}_{l_g t,k} + y^{out}_{l_g t,k})(y^{in}_{l_g t} + y^{out}_{l_g t})}{2} - \phi_{l_g} (u_{l^2_g t,k})^2 \\ & - \frac{(y^{in}_{l_g t,k} + y^{out}_{l_g t,k})^2}{4} + 2\phi_{l_g} u_{l^2_g t,k} u_{l^2_g t}, \ \forall l_g, t. \end{aligned} \tag{34}$$

Note that (34) is a set of convex quadratic inequalities and can be further converted to second-order cone (SOC) inequalities as follows [47]

$$x^2 \le by - d \Rightarrow \left\| \begin{array}{c} 2x \\ y - b \\ 2\sqrt{d} \end{array} \right\| \le y + b. \tag{35}$$

To make the linear approximations performed in (34) compatible, the nonnegative slack variable vector $\boldsymbol{s}$ as well as the penalty term associated with $\boldsymbol{s}$ are incorporated in constraint (34) and objective (31a), respectively, rendering a penalized version of CCP shown in Algorithm 1, which is able to find a local, but very promising to be the global, OGF solution. The convergence is proved in [46].

In Step 2 of Algorithm 1, problem (37), denoted as $\mathcal{M}^k_g$, is solved in its SOCP form using the transforation in (35). While Algorithm 1 converges, we solve the dual problem of $\mathcal{M}^k_g$ in the last iteration, which is again an SOCP, and recover dual variables $\varrho_{i_g t}$ as the LMGPs. The duality form of the SOCP is similar to (30) and is omitted here.

C. Market Equilibrium

Let OPF(LMGP, $\boldsymbol{y}$) (OGF(LMEP, $\boldsymbol{x}$)) be the OPF (OGF) problem with given LMGPs (LMEPs) and OGF (OPF) result $\boldsymbol{y}$ ($\boldsymbol{x}$), the equilibrium of the market with bilateral gas-electricity trading can come down to a fixed point problem

$$\begin{aligned} [\text{LMEP}, \boldsymbol{x}] &= \text{OPF}(\text{LMGP}, \boldsymbol{y}) \\ [\text{LMGP}, \boldsymbol{y}] &= \text{OGF}(\text{LMEP}, \boldsymbol{x}) \end{aligned} \tag{39}$$

The market interdependency originates from two observations: (i) the LMEPs (LMGPs), namely the dual variables of the OPF (OGF) problem, appear in the objective function of the OGF (OPF) problem; (ii) the gas (electricity) usage of gas-fired generators (compressors), i.e., the primal variables of the OPF (OGF) problem, appear in the constraints of the OGF (OPF) problem. A best-response decomposition algorithm is designed to identify the market equilibrium. Details are given in Algorithm 2.

Remark 7: In fact, the proposed model and solution methodology could extend to the cases with uncertain renewables in the PDN. Currently, two major modeling approaches are widely adopted in the power system operation problems with uncertain renewables, which are the scenario based stochastic approach and the uncertainty set based robust one.

(1) *Scenario based stochastic approach*: if uncertainty of renewables is represented by scenarios, and the goal of operator of the PDN is to minimize the expected operation costs, the compact form of the OPF problem would be a stochastic

programming as follows

$$\min_{\boldsymbol{x}^j} \sum_j \pi_j \left(\boldsymbol{f}^\top \boldsymbol{x}^j + \left(\boldsymbol{\varrho}^j\right)^\top \boldsymbol{F}_{\varrho x} \boldsymbol{x}^j \right) \quad (40a)$$

$$s.t.\ \mathbf{0} \le \boldsymbol{C}_1 \boldsymbol{x}^j + \boldsymbol{d}_1 + \boldsymbol{D}_1 \boldsymbol{y}^j + \boldsymbol{M}_1 \boldsymbol{u}^j : \boldsymbol{\beta}^j,\ \forall j, \quad (40b)$$

$$||\boldsymbol{A}_i \boldsymbol{x}^j + \boldsymbol{b}_i||_2 \le \boldsymbol{c}_{2,i}^\top \boldsymbol{x}^j + d_{2,i} : \boldsymbol{\delta}^j, \boldsymbol{\omega}^j,\ i \in L_p,\ \forall j, \quad (40c)$$

where j is scenario index and $\boldsymbol{u}^j$ is outputs of the renewables in scenario j; π_j is probability of scenario j; $\boldsymbol{x}^j$ is vector of decision variables in scenario j; $\boldsymbol{f}$, $\boldsymbol{F}_{\varrho x}$, $\boldsymbol{C}_1$, $\boldsymbol{d}_1$, $\boldsymbol{D}_1$, $\boldsymbol{M}_1$, $\boldsymbol{A}_i$, $\boldsymbol{b}_i$, $\boldsymbol{c}_{2,i}$, $d_{2,i}$ in model (40) are the same as model (29); $\boldsymbol{M}_1$ is the coefficient matrix for outputs of renewables; $\boldsymbol{\beta}^j, \boldsymbol{\delta}^j$ and $\boldsymbol{\omega}^j$ are dual variables. In problem (40), $\boldsymbol{y}^j$ and $\boldsymbol{\varrho}^j$ are constant electricity demands and LMGPs delivered from the GDN. In (40), the objective (40a) is to minimize the expected operation costs of the PDN, i.e., a weighted sum of the operation costs in each scenario; (40b) and (40c) are the PDN operation constraints in each scenario. With the integration of renewables in the PDN, uncertainty will impact the OGF problem indirectly, due to interdependencies between the PDN and the GDN, leading to a stochastic formulation of the OGF problem as follows

$$\min_{\boldsymbol{y}^j} \sum_j \pi_j \left(\boldsymbol{g}^\top \boldsymbol{y}^j + \left(\boldsymbol{\beta}^j\right)^\top \boldsymbol{G}_{\beta y} \boldsymbol{y}^j \right) \quad (41a)$$

$$s.t.\ \ \mathbf{0} \le \boldsymbol{E}\boldsymbol{y}^j + \boldsymbol{h} + \boldsymbol{H}\boldsymbol{x}^j :\ \boldsymbol{\varrho}^j,\ \forall j, \quad (41b)$$

$$\left(\boldsymbol{y}^j\right)^\top \boldsymbol{Q}\boldsymbol{y}^j = \mathbf{0},\ \forall j, \quad (41c)$$

where $\boldsymbol{y}^j$ is vector of decision variables in scenario j, and $\boldsymbol{g}, \boldsymbol{G}_{\beta y}$, $\boldsymbol{E}, \boldsymbol{h}, \boldsymbol{H}$ in (41) are the same as (31). $\boldsymbol{x}^j$ and $\boldsymbol{\beta}^j$ are constants delivered from the PDN. In (41), the objective (40a) is to minimize the expected operation costs of the GDN, i.e., a weighted sum of the operation costs in each scenario; (41b)-(41c) are GDN operation constraints in each scenario. Specially, (41c) represents the nonlinear Weymouth equation.

However, it should be noted that the mathematical properties of the stochastic OPF and OGF models are the same with corresponding deterministic ones, which are respectively SOCPs and quadratic equality constrained programmings. Therefore, the proposed solution approach would still work in this situation.

(2) *Uncertainty set based robust approach*: if uncertainty of renewables is represented by an uncertainty set, and the decision goal of the PDN operator is to evaluate the "worst-case" operation costs, the OPF problem would be a max-min programming as below

$$\max_{\boldsymbol{u}\in\mathcal{U}} \min_{\boldsymbol{x}}\ \boldsymbol{f}^\top \boldsymbol{x} + \boldsymbol{\varrho}^\top \boldsymbol{F}_{\varrho x} \boldsymbol{x} \quad (42a)$$

$$s.t.\ \mathbf{0} \le \boldsymbol{C}_1 \boldsymbol{x} + \boldsymbol{d}_1 + \boldsymbol{D}_1 \boldsymbol{y} + \boldsymbol{M}_1 \boldsymbol{u}\ :\ \boldsymbol{\beta}, \quad (42b)$$

$$||\boldsymbol{A}_i \boldsymbol{x} + \boldsymbol{b}_i||_2 \le \boldsymbol{c}_{2,i}^\top \boldsymbol{x} + d_{2,i}\ :\ \boldsymbol{\delta}, \boldsymbol{\omega},\ i \in L_p, \quad (42c)$$

where $\boldsymbol{u}$ is outputs of renewables; $\mathcal{U}$ is the predetermined uncertainty set; other notations are the same as (29). Obviously, (42) is not immediately solvable as it is a max-min programming. One widely adopted treatment is to take the dual of the inner level minimization problem, and then the bi-level programming would degenerate to a single level maximization problem with bilinear terms in the objective function. Big-M based linearization approach in [48] can be applied and the tractable reformulation is a mixed integer second-order cone programming (MISOCP), which can be solved by commercial solvers such as Gurobi. Then the "worst-case" realization of $\boldsymbol{u}$ can be obtained, denoted as $\boldsymbol{u}^*$, and the LMEPs $\boldsymbol{\beta}$ can be retrieved by substituting $\boldsymbol{u}^*$ into (29). It should be noted that the OGF problem will remain the same with (31), as both decision vector of PDN $\boldsymbol{x}$ and LMEPs $\boldsymbol{\beta}$ in the worst-case realization of $\boldsymbol{u}$ are deterministic values rather uncertain ones. And it is not hard to tell that the proposed approach would still work in this situation.

D. Discussions on the Existence of Market Equilibrium

Due to the complicated mathematical structure of the market equilibrium problem, provable convergence guarantee of Algorithm 2 is non-trivial. We provide some intuitive discussions to explain under what conditions Algorithm 2 is likely to converge or may fail to converge. Our analysis rests on the nodal price-demand curves.

Consider a PDN node i_p^*, which is connected with a gas-fired DG g^*, whose gas supply comes from GDN node i_g^*. The relationship between the gas demand of g^* and the gas price at i_g^* is illustrated by the grey curve in Fig. 2. While the gas price ρ is no larger than a certain value, say $\rho \le \rho_1$, DG g^* will keep working at its maximum generation capacity. It is also easy to image that if ϱ is greater than a certain value ϱ_2, g^* might lose all the energy contract. When $\varrho_1 \le \varrho \le \varrho_2$, the optimal generation of g^* is likely to be a continuously decreasing function in ϱ. Continuity is indicated by the fact that the Pareto-front of feasible nodal injection region for a radial network is strictly convex due to network losses, which is revealed in [49], [50].

Now we consider the price response from the GDN: the LMGP at node i_g^* is a function of the gas demand of g^*, which is plotted by black curves in Fig. 2. As mentioned before, the LMGPs can be decomposed into a purchase component which depends on the gas price at TLGM and a delivery component which relies on the LMEP at the compressor bus. Both of them are non-decreasing. When the demand exceeds the line pack capacity, the compressor has to increase its output in order to deliver more gas. As a result, the LMGP grows as the LMEP rises. However, the continuity of black curves depends on specific system data. If it is indeed continuous, it is very likely to intersect with the grey one. The intersection interprets the fixed point. If it is discontinuous, an intersection point may exist or may not exist, as illustrated in Fig. 2.

Similarly, we consider a GDN node with a compressor c^*, whose electricity is supplied by PDN bus i_p^*. The relationship between the electricity demand of c^* and the LMEP at i_p^* is portrayed by grey curves in Fig. 3. The demand of c^* remains unchanged as long as the value of LMEP $\beta_{i_p^*}$ is either small or large enough. Grey curves can be either continuous or discontinuous, depending on the data of the OGF problem. On the other hand, black curves in Fig. 3 depict the LMEP as a function of electricity demand of c^*. In general, an LMEP curve would be discontinuous, because nodal price could be attributed to a number of factors, and any active inequality might introduce a sudden rise in the LMEP. Take the lossless power transmission network for example, the nodal price is

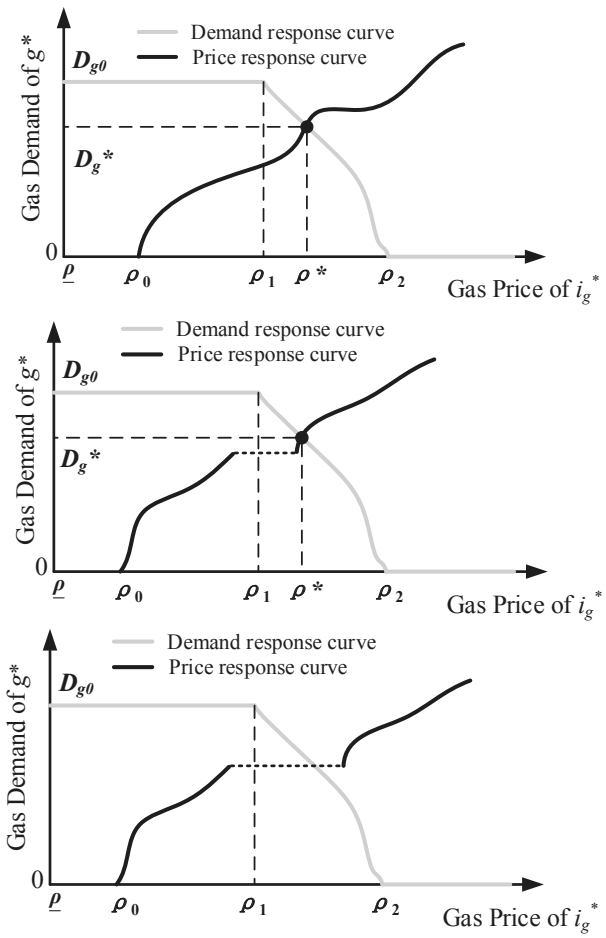

Fig. 2. Illustration of gas price and gas demand curves.

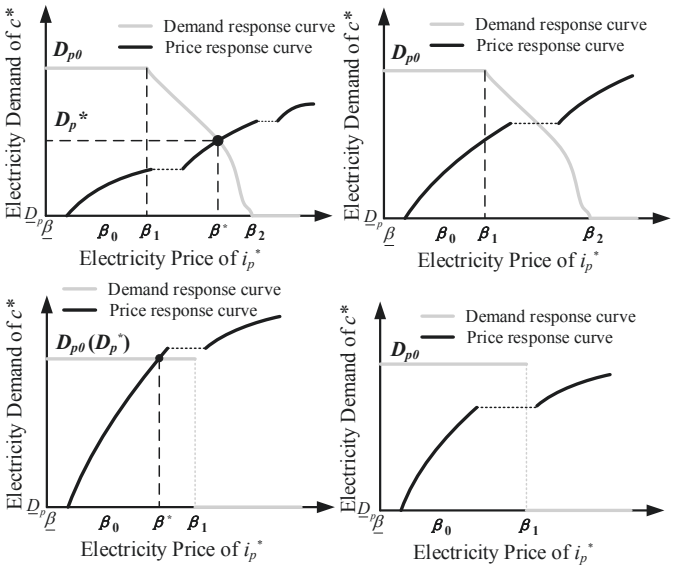

Fig. 3. Illustration of electricity price and electricity demand curves.

known to be stepwise constant [51]. Fig. 3 demonstrates four possible outcomes. In each of the left two subfigures, the two curves have an intersection, and the market equilibrium exists; in the right two subfigures, no equilibria exist.

From above discussions, it can be concluded that the existence of market equilibrium is system dependent. If no equilibrium exists, Algorithm 2 will fail to converge. In continuous case, Algorithm 2 is very likely to converge and find the equilibrium, regardless of the initial point; If either of the curves is discontinuous, the equilibrium may not exist. In addition, even if an equilibrium indeed exists, whether Algorithm 2 can converge depends on the selection of the initial point.

IV. Illustrative Example

In this section, we present numerical results on two test systems to validate the proposed methods. All experiments are performed on a laptop with Intel(R) Core(TM) 2 Duo 2.2 GHz CPU and 4 GB memory. The proposed algorithms are coded in MATLAB with YALMIP toolbox [52]. SOCPs are solved by Gurobi 6.5.

Fig. 4 depicts the topology of the connected infrastructures, which will be referred to as the Power13Gas7 system later on. The PDN has 2 gas-fired DGs and 8 electric loads. The GDN possesses 2 compressors, 4 passive pipelines, and 6 gas loads. In Fig. 4, P, PL, and DG with subscripts denote electrical buses, power loads, and DG units in the PDN, respectively; N, C, GL, and $GLine$ with subscripts denote gas nodes, compressors, gas loads, and passive pipelines in GDN, respectively. Specially, the fuel of DG_1 and DG_2 are supplied by GDN nodes N_4 and N_6, respectively. Electrical compressors C_1 and C_2 are connected to PDN buses P_3 and P_8, respectively. The daily demand profiles and price forecasts in TLEM and TLGM are shown in Fig. 5 and Fig. 6. Other detailed system data are available in [53]. Hereinafter, we use the million British thermal unit (MMBtu) as the unifying unit for electricity and natural gas, i.e., 1MMBtu equals to the thermal energy of 28.3 Sm^3 thorough burnt gas, or 293 kWh electricity.

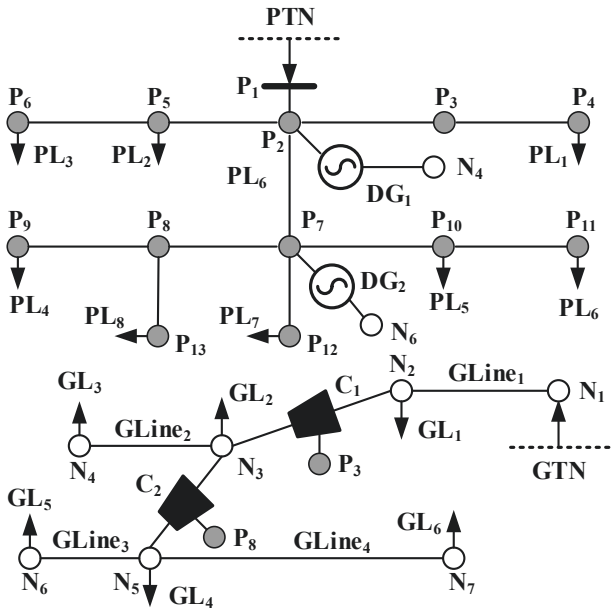

Fig. 4. Topology of the Power13Gas7 system.

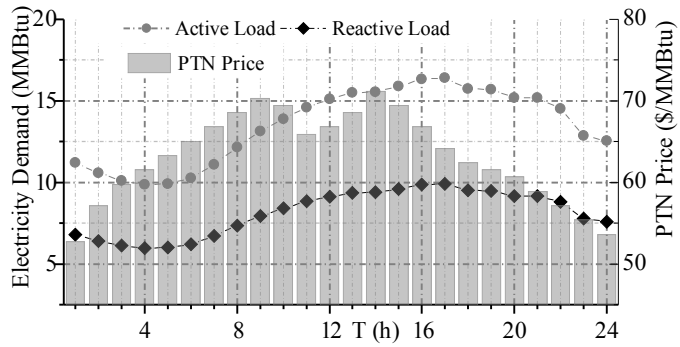

Fig. 5. Demand profile of the PDN and the price curve in the TLEM.

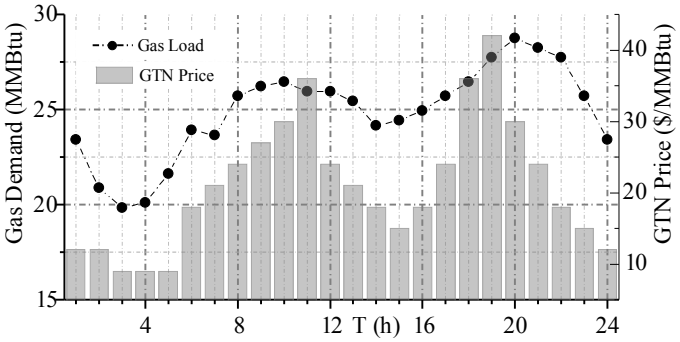

Fig. 6. Demand profile of the GDN and the price curve in the TLGM.

A. Simulation Results of the Base Case

The initialization parameters of Algorithm 1 and Algorithm 2 are provided in Table I. Algorithm 1 for the OGF problem always converges in 3 iterations in our tests. Algorithm 2 identifies the market equilibrium after 4 iterations. Hourly LMEPs and LMGPs are plotted in Fig. 7 and Fig. 8, respectively. From Fig. 7, it can be observed that the LMEP curve at the slack bus is identical with the given price curve in Fig. 5, and the LMEPs of other buses in the same time period grow with increasing distances to the slack bus, due to the unilateral power flows and network losses. In particular, the hourly LMEP curve at each bus has a shape similar to the price curve in Fig. 5. In fact, among various factors that would possibly influence nodal prices including network losses, congestions, and bus voltage limits, network losses impacts the LMEPs in distribution networks more evidently than it does in transmission networks, where the line resistance to reactance ratio is much smaller, and all buses share only one marginal cost in the absence of congestions. This result indicates that the lossless power flow model, such as the direct current power flow model which has been widely used in transmission-level studies, and the linearized branch flow model [54] which is also popular in distribution-level studies, may be less accurate for calculating the LMEPs in distribution networks.

Because the node connected with the TLGM is the only gas source, and gas delivery may incur electricity consumption, the LMGPs are affected by the following two factors: the gas price in the TLGM and LMEPs corresponding to active pipelines (compressors). As a result, the LMGP curve is stepwise constant with respect to node index, as demonstrated in Fig. 8. Moreover, it can be observed that the LMGP curves at N_1 and N_2 do not change over time, and fluctuations in the LMGP curves at other gas nodes are smaller than the price variation trend shown in Fig. 6, due to the line pack effect, which can be regarded as a sort of gas storage, allows the GDN operator purchase and store extra gas when the price in the TLGM is low. In this case, the line pack capacity of $GLine_1$ is adequate to store the gas which is purchased during periods 3 to 5 with the lowest gas prices, contributing to the constant hourly LMGP curves at nodes N_1 and N_2. For N_3 and N_5, they are downstream nodes of active pipelines C_1 and C_2, respectively, and their hourly LMGP curves share similar variation patterns with hourly LMEP curves of their electricity supply nodes P_3 and P_8, respectively, since active pipelines do not have line pack effect, and delivery costs for N_3 and N_5 are directly related to LMEPs at P_3 and P_8. For N_4, N_6, and N_7, extra gas purchased in low-price periods can be stored in $GLine_2, GLine_3$, and $GLine_4$, respectively, which results in lower LMGPs compared with those at N_3 and N_5, respectively.

TABLE I
PARAMETERS OF ALGORITHM 1 AND ALGORITHM 2

Algorithm 1						Algorithm 2	
δ	π_0	π_{max}	ε	κ	k^{max}	ϵ	j^{max}
1	0.01	1000	10^{-6}	2	20	10^{-4}	20

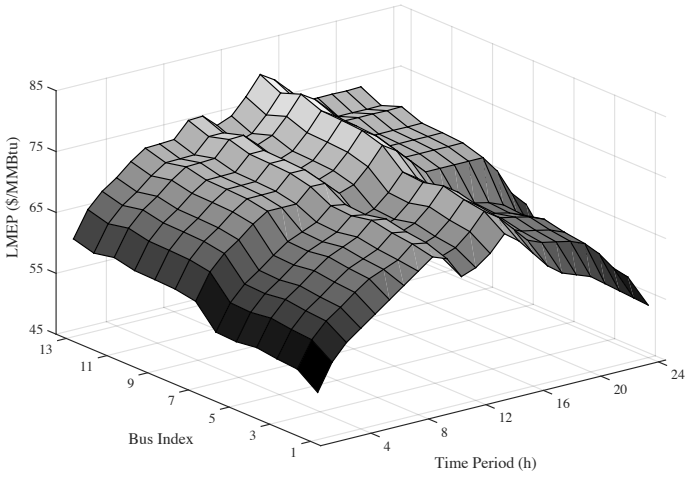

Fig. 7. The LMEP curves of the PDN.

B. Impacts of the Line Pack Effect

In this subsection, the line pack in passive pipelines is neglected, which is implemented by dropping $m_{l_g t}$ and constraints (16)-(17) in the OGF problem. Operating costs of the PDN and the GDN at market equilibrium are listed in Table II, which are increased by 20.3% and 97.1%, respectively, compared with those in the base case. From previous results, the economic benefits of line pack effect is clear: it helps reduce energy prices and system operation costs by allowing more flexible gas transactions between GDN and TLGM.

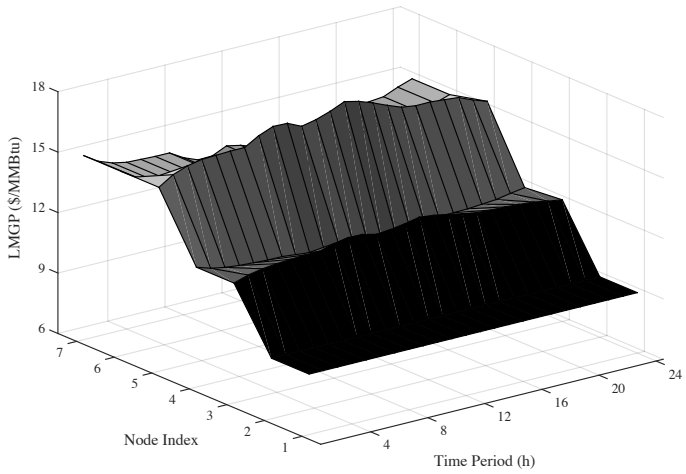

Fig. 8. The LMGP curves of the GDN.

TABLE II
OPERATING COSTS AT EQUILIBRIUM WITH/WITHOUT LINE PACK

	PDN ($)	GDN ($)
With line pack	2.1505×10^4	7.6052×10^4
Without line pack	2.5871×10^4	1.4990×10^5

In fact, the line pack capacity in the pipelines are mainly determined by nodal pressure limits and parameters of the pipelines. And nodal pressure limits are crucial to both the operating feasibility and flexibility of the GDN. From the feasibility perspective, if the limits decrease, the maximum allowable gas flow through a pipeline would decrease simultaneously, and if the limits are below certain thresholds, the nodal gas balancing equations would not hold, leading to infeasibility issues of the OGF problem. And from the flexibility perspective, capacity of the line pack has a positive relationship with pressures of head and tail nodes of a pipeline according to (16), which means it will drop correspondingly if the pressure limits decrease. And of course the lower line pack capacities are, the higher the operation costs of both energy distribution networks might be, indicating lower operating flexibility of the GDN accordingly. To verify the aforementioned analysis, the simulations in Section IV.A are repeated with different nodal pressure limits, and operation costs of the two energy networks are displayed as follows

TABLE III
OPERATING COSTS AT EQUILIBRIUM WITH DIFFERENT LEVELS OF NODAL PRESSURE LIMITS.

Pressure (%)	PDN ($)	GDN ($)
100	2.1505×10^4	7.6052×10^4
80	2.2201×10^4	8.3217×10^4
60	2.3445×10^4	9.7762×10^4
40	2.5162×10^4	1.2165×10^5
20	-	Infeasible

In Table III, the left column indicates pressure limits level, e.g., 80% means pressure limits of all nodes are 80% of the corresponding values in the Power13Gas7 test system. From Table III, it can be observed that operation costs of both energy networks will increase along with the drop of pressure limits. Specifically, when pressure limits drop to 20%, the OGF problem would be infeasible.

C. Comparisons with other OGF Solution Methods

As previously mentioned, the sequential SOCP algorithm is proposed to solve the gas market clearing problem, which identifies a local, but very promising to be the global, OGF solution. In fact, due to the nonlinearities and nonconvexities in the gas market clearing problem, the global optimality of the solution cannot be theoretically guaranteed. However, it is still worth comparing the quality of the solution obtained by the proposed algorithm with the ones obtained by other algorithms and methods. To the best knowledge of the authors, three methods to solve the nonlinear and nonconvex OGF problem have been reported by the literature, which are

1) A1: MILP based method [10]–[14], where the nonlinear Weymouth equation is approximated by a series of linear segments and nearly same amount of binary variables are added, rendering an MILP approximation of the original OGF problem.
2) A2: SOCP/ linear programming (LP) relaxation method [2], [5], where the Weymouth equation is relaxed as an SOCP inequality or a series of linear inequalities, transforming the nonconvex OGF problem into a convex one.
3) A3: Interior point method, which can obtain a solution for many nonlinear programming in a given time limit. It should be noted the initial point have direct impact on the quality of solution.

The gas network of the Power13Gas7 system is selected as the test system for the OGF problem. The parameters can be found in [53]. The variables, which are related to the electricity network and appear in the OGF problem, are parameterized with the OPF solution in the last iteration of Algorithm 2. In A1, two eight-segment piecewise linear approximations are adopted to replace the nonlinear Weymouth equation [11]. To test the performance of A3 under different choices of initial point, A3 is performed 10^3 times with different initial points, including the OGF solution offered by A2, which is identical with the initial point of CCP. Particularly, MILPs are solved by Gurobi 6.5 and the interior point method is from OPTI toolbox. The solution time limit is set as 10 minutes. The simulation results are summarized in Table IV, where F, Y and N are short for feasible, yes and no, respectively, in the fifth column.

TABLE IV
COMPARISON WITH THE STATE-OF-ART METHODOLOGIES FOR THE OGF PROBLEM

	Objective ($)			F	Time (s)
	avg	max	min		
CCP	7.605×10^4	-	-	Y	0.68
A1	8.426×10^4	-	-	Y	720*
A2	7.405×10^4	-	-	N	0.09
A3	7.824×10^4	8.294×10^4	7.652×10^4	Y	75

The comparisons are conducted in three aspects, namely, the OGF costs, the feasibility of the OGF solution, and the solution

time. It should be noted that, the results of CCP, A1, and A2 in Table IV refer to the single time performance of these algorithms, while the results of A3 is the average performance of 10^3 tests. From Table IV, though the objective value of A2 is the lowest, its OGF solution is infeasible. A1 can offer a feasible solution, however, its computational burden is the largest and the time runs out before an optimal solution is obtained. Among the algorithms which can offer a feasible OGF solution, namely, CCP, A1 and A3, CCP performs the best in terms of both objective value and solution time. From the simulation results, it should be noted that OGF solution offered by CCP is always better than A3, including the best case of A3. In this regard, the OGF solution offered by the proposed CCP method is satisfying, which is the basis of an "optimal" equilibrium.

D. Impacts of Compressors

If the GDN in the couple energy networks does not have compressor stations, the models and algorithms still work after the following modifications

1) In the PDN market clearing model, remove the active power consumption terms of the compressor in the nodal active power balance equation.
2) In the GDN market clearing model, remove the electricity purchase cost terms in the objective function as well as the compressor related terms and models in the constraints.
3) In the proposed best-response decomposition algorithm, remove the compressor related convergence criterion.

To demonstrate the impact of compressors on the results, numerical tests are executed on the modified Power13Gas7 system, where the compressors in the GDN have been removed, and the rest is the same as the Power13Gas7 system demonstrated in Section IV, including the daily electricity demand profiles and price forecasts in the transmission-level energy markets. It should be noted that the OGF problem would be infeasible without compressors, if the daily gas demand profiles stay the same. Therefore, the gas demands are set as one third of the ones in [53] to recover the feasibility of the OGF problem with no compressors equipped.

Likewise, Algorithm 1 for the OGF problem always converges in 3 iterations. And Algorithm 2 locates the market equilibrium after 3 iterations, which converges faster than the case in Section IV.A, because the bilateral energy trading degenerates to unilateral one, as a result, the interdependency is weakened. Hourly LMGPs are shown in Fig. 9. From Fig. 9, it can be observed that the LMGPs remain unchanged throughout the day, and their values are 9 \$/MMBtu, which is the lowest price of TLGM. The reason is that the GDN operation costs only consist of the gas purchase costs from the GTN as there is no compressors, and the pipelines are capable to store adequate gas when the price is low. Though the LMGPs have decreased dramatically compared with the case in Section IV.A, the LMEP curves in this case share the same trends as Fig.7. This is because the total capacity of DGs in the PDN is always smaller than its hourly electricity demand, which indicates the PDN has to buy electricity from the PTN invariably in both cases. In the case of Section IV.A, PTN is the marginal "generator", as its price is the higher than the DGs. In this case, the generation costs of DGs decrease as the LMGPs decrease, which means the PTN is still the marginal "generator", resulting in the same variation trends in the LMEP curves of the two cases.

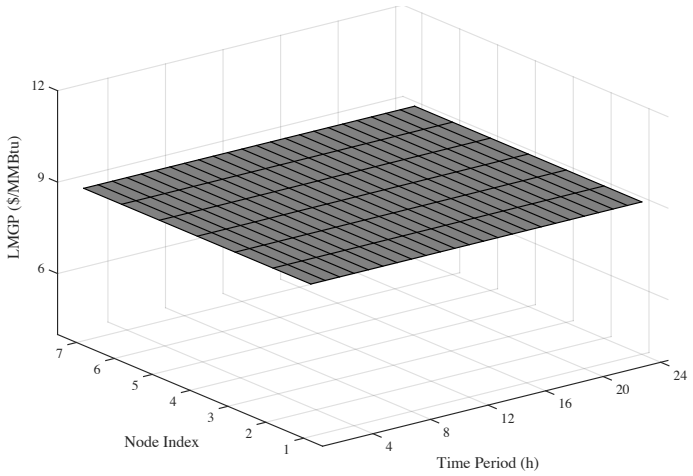

Fig. 9. The LMGP curves of the GDN with no compressors equipped.

E. Computational Efficiency Analysis

To demonstrate the scalability and efficiency of the proposed methods, they are applied to a larger system, consisting of a modified IEEE 123-bus power feeder and a modified Belgian high-calorific 20-node gas network, which will be referred to as the Power123Gas20 system hereinafter. The system includes 10 gas-fired DGs, 3 compressors, 16 passive pipelines, 85 power loads, and 9 gas loads. Please refer to [53] for the network topology, the demand curves as well as other system data. Algorithmic parameters in Table I are used in this case.

The convergence performances are shown in Fig. 10. It can be observed that both algorithms converge in 3 iterations. The total computation time of Algorithm 1 and Algorithm 2 is 7.24 seconds, demonstrating the scalability of the proposed methods. Besides the satisfactory convergence rates of Algorithms 1-2, the high efficiency is also attributed to the computational superiority of SOCPs, which can be readily solved even for very large-scale instances [47].

V. Conclusion

The interdependencies between power systems and gas systems have been greatly enhanced in recent decades, indicating a greater amount of bilateral energy flows as well as more business opportunities. In this paper, a market framework for the coupled power and gas distribution systems, both with radial topologies, is designed, which allows the energy markets to trade energy bilaterally with its marginal price. Under certain assumptions and simplifications, the multi-period alternating current OPF problem becomes tractable using convex relaxation techniques. The penalty CCP algorithm is developed to turn the nonlinear and nonconvex multi-period OGF problem with the line pack effect into a tractable one,

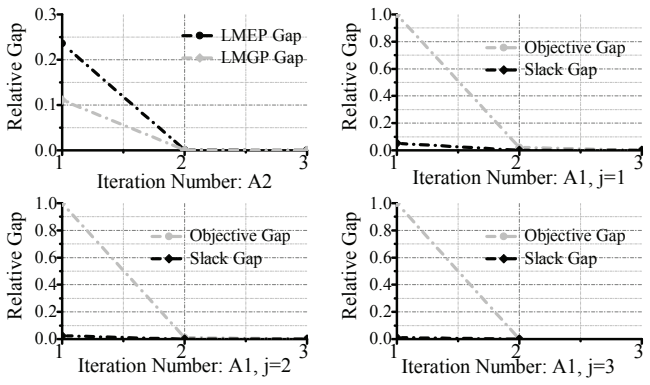

Fig. 10. Algorithm performances in the Power123Gas20 system.

where a sequence of convex optimization problems is tackled. SOCP based methods are used to solve the OPF problem and the OGF problem, as well as to recover the locational marginal energy prices. A best-response decomposition algorithm is developed to identify the market equilibrium, whose existence is analytically investigated via nodal price-demand curves. Simulation results corroborate the effectiveness of the proposed methods, and reveal economic benefits of the line pack effect. Two promising aspects are selected as our future research interests and listed as below, which could facilitate the application of the proposed market framework.

1) More accurate and tractable gas network modelling. Detailed compressor models would be considered. The accuracies of the approximation techniques for the gas flows and their dynamics need to be improved.
2) More reliable algorithm for market equilibrium identification. Particularly, a criterion for the existence of the market equilibrium needs to be developed.

ACKNOWLEDGMENT

The authors would like to thank the editor and six anonymous reviewers for their valuable and inspiring suggestions to improve the quality of the paper.

REFERENCES

[1] A. Martinez-Mares and C. Fuerte-Esquivel, "A unified gas and power flow analysis in natural gas and electricity coupled networks," *IEEE Trans. Power Syst.*, vol. 27, no. 4, pp. 2156–2166, Nov. 2012.

[2] L. Bai, F. Li, H. Cui, T. Jiang, H. Sun, and J. Zhu, "Interval optimization based operating strategy for gas-electricity integrated energy systems considering demand response and wind uncertainty," *Appl. Energy*, vol. 167, pp. 270–279, Apr. 2016.

[3] C. Liu, M. Shahidehpour, and J. Wang, "Coordinated scheduling of electricity and natural gas infrastructures with a transient model for natural gas flow," *Chaos: An Interdisciplinary Journal of Nonlinear Science*, vol. 21, no. 2, p. 21052, 2011.

[4] X. Zhang, M. Shahidehpour, A. Alabdulwahab, and A. Abusorrah, "Security-constrained co-optimization planning of electricity and natural gas transportation infrastructures," *IEEE Trans. Power Syst.*, vol. 30, no. 6, pp. 2984–2993, Nov. 2015.

[5] H. Cui, F. Li, Q. Hu, L. Bai, and X. Fang, "Day-ahead coordinated operation of utility-scale electricity and natural gas networks considering demand response based virtual power plants," *Appl. Energy*, vol. 6, pp. 183–195, Aug. 2016.

[6] A. Tomasgard, F. Rmo, M. Fodstad, and K. Midthun, "Optimization Models for the Natural Gas Value Chain," in *Geometric Modelling, Numerical Simulation, and Optimization: Applied Mathematics at SINTEF*. Berlin, Heidelberg: Springer, 2007, pp. 521–558.

[7] R. Chen, J. Wang, and H. Sun. (2016) Clearing and pricing for coordinated gas and electricity day-ahead markets considering wind power uncertainty. [Online]. Available: https://arxiv.org/abs/1611.09599

[8] M. Gil, P. Dueñas, and J. Reneses, "Electricity and natural gas interdependency: comparision of two methodologies for coupling large market models within the european regulatory framework," *IEEE Trans. Power Syst.*, vol. 31, no. 1, pp. 361–369, Jan. 2016.

[9] C. Wang, W. Wei, J. Wang, L. Bai, Y. Liang, and T. Bi, "Convex optimization based distributed optimal gas-power flow calculation," *IEEE Trans. Sustain. Ener.*, vol. PP, no. 99, pp. 1–1, 2017.

[10] C. M. Correa-Posada and P. Snchez-Martn, "Security-constrained optimal power and natural-gas flow," *IEEE Trans. Power Syst.*, vol. 29, no. 4, pp. 1780–1787, July 2014.

[11] C. Correa-Posada and P. Sanchez-Martin, "Integrated power and natural gas model for energy adequacy in short-term operation," *IEEE Trans. Power Syst.*, vol. 30, no. 6, pp. 3347–3355, Nov. 2015.

[12] C. Wang, W. Wei, J. Wang, F. Liu, F. Qiu, C. M. Correa-Posada, and S. Mei, "Robust defense strategy for gas-electric systems against malicious attacks," *IEEE Trans. Power Syst.*, vol. 32, no. 4, pp. 2953–2965, July 2017.

[13] C. He, L. Wu, T. Liu, and M. Shahidehpour, "Robust co-optimization scheduling of electricity and natural gas systems via ADMM," *IEEE Trans. Sustain. Ener.*, vol. 8, no. 2, pp. 658–670, 2017.

[14] C. Shao, X. Wang, M. Shahidehpour, X. Wang, and B. Wang, "An milp-based optimal power flow in multicarrier energy systems," *IEEE Trans. Sustain. Ener.*, vol. 8, no. 1, pp. 239–248, Jan 2017.

[15] D. A. Schiro, T. Zheng, F. Zhao, and E. Litvinov, "Convex hull pricing in electricity markets: Formulation, analysis, and implementation challenges," *IEEE Trans. Power Syst.*, vol. 31, no. 5, pp. 4068–4075, Sep 2016.

[16] B. Hua and R. Baldick, "A convex primal formulation for convex hull pricing," *IEEE Trans. Power Syst.*, vol. 32, no. 5, pp. 3814–3823, Sep. 2017.

[17] P. Weigand, G. Lander, and R. Malme, "Synchronizing natural gas & power market: a series of proposed solutions," Skipping Stone, Tech. Rep., Jan. 2013.

[18] "Analysis of operational events and market impacts during the january 2014 cold weather events," PJM Interconnection, Tech. Rep., May 2014.

[19] G. Li, R. Zhang, T. Jiang, H. Chen, L. Bai, and X. Li, "Security-constrained bi-level economic dispatch model for integrated natural gas and electricity systems considering wind power and power-to-gas process," *Appl. Energy*, vol. 194, pp. 696–704, May 2017.

[20] C. Ruiz, A. J. Conejo, and Y. Smeers, "Equilibria in an oligopolistic electricity pool with stepwise offer curves," *IEEE Trans. Power Syst.*, vol. 27, no. 22, pp. 752–761, May 2012.

[21] M. E. Baran and F. F. Wu, "Network reconfiguration in distribution systems for loss reduction and load balancing," *IEEE Trans. Power Deliver.*, vol. 4, no. 2, pp. 1401–1407, Apr. 1989.

[22] M. Farivar and S. H. Low, "Branch flow model: Relaxations and convexification," *IEEE Trans. Power Syst.*, vol. 28, no. 3, pp. 2554–2572, Aug. 2013.

[23] K. Christakou, D.-C. Tomozei, J.-Y. L. Boudec, and M. Paolone, "Ac opf in radial distribution networks part i: On the limits of the branch flow convexification and the alternating direction method of multipliers," *Electric Power Systems Research*, vol. 143, pp. 438 – 450, 2017.

[24] M. Nick, R. Cherkaoui, J. Y. LeBoudec, and M. Paolone, "An exact convex formulation of the optimal power flow in radial distribution networks including transverse components," *IEEE Trans. Automat. Contr.*, vol. PP, no. 99, pp. 1–1, 2017.

[25] L. Gan, N. Li, U. Topcu, and S. H. Low, "Exact convex relaxation of optimal power flow in radial networks," *IEEE Trans. Automat. Contr.*, vol. 60, no. 1, pp. 72–87, Jan 2015.

[26] R. Fernández-Blanco, J. Arroyo, and N. Alguacil, "On the solution of revenue- and network-constrained day-ahead market clearing under marginal pricing - part I: an exact bilevel programming approach," *IEEE Trans. Power Syst.*, vol. 32, no. 1, pp. 208–219, Jan. 2017.

[27] J. Lavaei and S. H. Low, "Zero duality gap in optimal power flow problem," *IEEE Trans. Power Syst.*, vol. 27, no. 1, pp. 92–107, Feb. 2012.

[28] J. Qiu, H. Yang, Z. Y. Dong, J. H. Zhao, K. Meng, F. J. Luo, and K. P. Wong, "A linear programming approach to expansion co-planning in gas and electricity markets," *IEEE Trans. Power Syst.*, vol. 31, no. 5, pp. 3594–3606, Sept 2016.

[29] C. Wang, W. Wei, J. Wang, F. Liu, and S. Mei, "Strategic offering and equilibrium in coupled gas and electricity markets," *IEEE Trans. Power Syst.*, vol. 33, no. 1, pp. 290–306, Jan. 2018.

[30] C. Liu, M. Shahidehpour, Y. Fu, and Z. Li, "Security-constrained unit commitment with natural gas transmission constraints," *IEEE Trans. Power Syst.*, vol. 24, no. 3, pp. 1523–1536, Aug. 2009.

[31] G. Li, R. Zhang, T. Jiang, H. Chen, L. Bai, and X. Li, "Security-constrained bi-level economic dispatch model for integrated natural gas and electricity systems considering wind power and power-to-gas process," *Appl. Energy*, vol. 194, pp. 696 – 704, 2017.

[32] C. Borraz-Snchez and R. Ros-Mercado, "Improving the operation of pipeline systems on cyclic structures by tabu search," *Computers and Chemical Engineering*, vol. 33, pp. 58–64, 2009.

[33] S. Wu, R. Ros-Mercado, E. Boyd, and L. Scott, "Model relaxations for the fuel cost minimization of steady-state gas pipeline networks," University of Chicago, Tech. Rep., 1999.

[34] J. Andre. (2010) Optimization of investments in gas networks. [Online]. Available: https://tel.archives-ouvertes.fr/tel-00539689

[35] R. Carvalho, L. Buzna, F. Bono, E. Gutiérrez, W. Just, and D. Arrowsmith, "Robustness of trans-european gas networks," *Phys. Rev. E*, vol. 80, p. 016106, Jul 2009.

[36] I. Mahdavi, N. Mahdavi-Amiri, A. Makui, A. Mohajeri, and R. Tafazzoli, "Optimal gas distribution network using minimum spanning tree," in *2010 IEEE 17Th International Conference on Industrial Engineering and Engineering Management*, Oct 2010, pp. 1374–1377.

[37] A. Mohajeri, I. Mahdavi, and N. Mahdavi-Amiri, "Optimal pipe diameter sizing in a tree-structured gas network: a case study," *International Journal of Industrial and Systems Engineering*, vol. 12, no. 3, pp. 346–368, 2012.

[38] A. Mohajerir, I. Mahdavi, N. Mahdavi-Amiri, and R. Tafazzoli, "Optimization of tree-structured gas distribution network using ant colony optimization: A case," *International Journal of Engineering*, vol. 25, no. 2, pp. 141–158, 2012.

[39] N. Shiono and H. Suzuki, "Optimal pipe-sizing problem of tree-shaped gas distribution networks," *Euro. Journal of Oper. Res.*, vol. 252, no. 2, pp. 550 – 560, 2016.

[40] K. Dvijotham, M. Vuffray, S. Misra, and M. Chertkov. (2015) Natural gas flow solutions with guarantees: A monotone operator theory approach. [Online]. Available: https://arxiv.org/abs/1506.06075

[41] R. Z. Ros-Mercado and C. Borraz-Snchez, "Optimization problems in natural gas transportation systems: A state-of-the-art review," *Appl. Energy*, vol. 147, pp. 536 – 555, 2015. [Online]. Available: http://www.sciencedirect.com/science/article/pii/S0306261915003013

[42] (2015) Natural gas infrastructure. Department of Energy. [Online]. Available: https://energy.gov/sites/prod/files/2015/06/f22/Appendix%20B-%20Natural%20Gas_1.pdf

[43] J. Yang, N. Zhang, C. Kang, and Q. Xia, "Effect of natural gas flow dynamics in robust generation scheduling under wind uncertainty," *IEEE Trans. Power Syst.*, vol. PP, no. 99, pp. 1–1, 2017.

[44] S. Acha and C. Hernandez-Aramburo, "Integrated modelling of gas and electricity distribution networks with a high penetration of embedded generation," in *CIRED Seminar 2008: SmartGrids for Distribution*, June 2008, pp. 1–4.

[45] C. Segeler, *Gas Engineers Handbook*. USA: Industrial Press, 1968.

[46] T. Lipp and S. Boyd, "Variations and extension of the convex-concave procedure," *Optim. Eng.*, vol. 17, pp. 263–287, 2016.

[47] M. S. Lobo, L. Vandenberghe, S. Boyd, and H. Lebret, "Applications of second-order cone programming," *Linear Algebra Appl.*, vol. 284, no. 1, pp. 193–228, Nov. 1998.

[48] L. Zhao and B. Zeng, "Robust unit commitment problem with demand response and wind energy," in *2012 IEEE Power and Energy Society General Meeting*, July 2012, pp. 1–8.

[49] B. Zhang and D. Tse, "Geometry of injection regions of power networks," *IEEE Trans. Power Syst.*, vol. 28, no. 2, pp. 788–797, May 2013.

[50] J. Lavaei, D. Tse, and B. Zhang, "Geometry of power flows and optimization in distribution networks," *IEEE Trans. Power Syst.*, vol. 29, no. 2, pp. 572–583, 2014.

[51] F. Li, "Continuous locational marginal pricing (clmp)," *IEEE Trans. Power Syst.*, vol. 22, no. 4, pp. 1638–1646, Nov. 2007.

[52] J. Löfberg, "YALMIP : A toolbox for modeling and optimization in matlab," in *In Proceedings of the CACSD Conference*, Taipei, Taiwan, 2004, pp. 284–289.

[53] (2016). [Online]. Available: https://sites.google.com/site/chengwang0617/home/data-sheet

[54] H.-G. Yeh, D. F. Gayme, and S. H. Low, "Adaptive VAR control for distribution circuits with photovoltaic generators," *IEEE Trans. Power Syst.*, vol. 27, no. 3, pp. 1656–1663, Aug. 2012.

Cheng Wang received the B.Sc. and Ph.D. degrees in electrical engineering from Tsinghua University, Beijing, China, in 2012 and 2017, respectively.

Dr. Wang was a Visiting Ph.D. student at Argonne National Laboratory, Argonne, IL, USA, from 2015 to 2016. He is currently a Lecturer with North China Electric Power University, Beijing, China. His research interests include optimization and control of integrated energy systems. He was an *"Outstanding Reviewer"* for IEEE Transactions on Power Systems in 2016.

Wei Wei (M'15) received the B.Sc. and Ph.D. degrees in electrical engineering from Tsinghua University, Beijing, China, in 2008 and 2013, respectively.

Dr. Wei was a Postdoctoral Research Fellow with Tsinghua University from 2013 to 2015. He was a Visiting Scholar with Cornell University, Ithaca, NY, USA, in 2014, and with Harvard University, Cambridge, MA, USA, in 2015. He is currently a Research Assistant Professor with Tsinghua University. His research interests include applied optimization and energy economics.

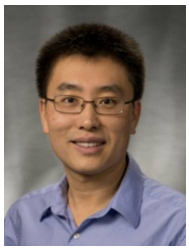

Jianhui Wang (M'07-SM'12) received the Ph.D. degree in electrical engineering from Illinois Institute of Technology, Chicago, Illinois, USA, in 2007.

Presently, he is an Associate Professor with the Department of Electrical Engineering at Southern Methodist University, Dallas, Texas, USA. He also holds a joint appointment as Section Lead for Advanced Power Grid Modeling at the Energy Systems Division at Argonne National Laboratory, Argonne, Illinois, USA.

Dr. Wang is the secretary of the IEEE Power & Energy Society (PES) Power System Operations, Planning & Economics Committee. He is an associate editor of Journal of Energy Engineering and an editorial board member of Applied Energy. He has held visiting positions in Europe, Australia and Hong Kong including a VELUX Visiting Professorship at the Technical University of Denmark (DTU). Dr. Wang is the Editor-in-Chief of the IEEE Transactions on Smart Grid and an IEEE PES Distinguished Lecturer. He is also the recipient of the IEEE PES Power System Operation Committee Prize Paper Award in 2015.

Lei Wu (SM'13) received the B.S. degree in electrical engineering and the M.S. degree in systems engineering from Xi'an Jiaotong University, Xi'an, China, in 2001 and 2004, respectively, and the Ph.D. degree in electrical engineering from Illinois Institute of Technology (IIT), Chicago, IL, USA, in 2008.

From 2008 to 2010, he was a Senior Research Associate with the Robert W. Galvin Center for Electricity Innovation, IIT. He worked as summer Visiting Faculty at NYISO in 2012. Currently, he is an Associate Professor with the Electrical and Computer Engineering Department, Clarkson University, Potsdam, NY, USA. His research interests include power systems operation and planning, energy economics, and community resilience microgrid.

Yile Liang (S'15) received the B.Sc. degree in electrical engineering from Huazhong University of Science and Technology, Wuhan, China, in 2012. Currently, she is pursing the Ph.D. degree in electrical engineering in Tsinghua University, Beijing, China.

Her research interests include distributed optimization of integrated energy systems.